表1　慢性肝炎の線維化分類

score	新犬山分類	modified HAI staging	HAI (fibrosis)	Ishak et al.	METAVIR system
0	線維化なし	No fibrosis	No fibrosis	No fibrosis	No fibrosis
1	門脈域の線維性拡大	Fibrous expansion of some portal areas, with or without short fibrous septa	Fibrous portal expansion	Mild fibrosis	Periportal fibrosis expansion
2	bridging fibrosis（線維性架橋形成）	Fibrous expansion of most portal areas, with or without short fibrous septa	-	Moderate fibrosis	P-P septae (>1 septum)
3	小葉のひずみを伴う bridging fibrosis	Fibrous expansion of most portal areas with occasional portal to portal (P-P) bridging	Bridging fibrosis (portal-portal or portal-central linkage)	Severe fibrosis	P-C septae
4	肝硬変	Fibrous expansion of portal areas with marked bridging [portal to portal (P-P) as well as portal to central (P-C)]	Cirrhosis	Cirrhosis	Cirrhosis
5		Marked bridging (P-P and / or P-C) with occasional nodules (incomplete cirrhosis)			
6		Cirrhosis, probable or definite			

肝炎の客観的評価に利用されてきた(表1).

1990年代に入り，C型肝炎の診断が容易になると，C型肝炎自体の診断，病理学的評価が可能となり，さらにアルコール性肝障害や脂肪肝との鑑別も明確となった．その結果，慢性肝炎の組織診断基準の見直しが行われるようになり，HAIスコアリング以外にさまざまな組織評価法の提唱がなされた[6]．1991年にScheuerら[7]が炎症の活動性と線維化を分けた分類を示し，1994年にはDesmetら[8]により新ヨーロッパ分類がまとめられた．同じ年，フランスの研究グループからもC型肝炎組織の評価法(METAVIRシステム)が提唱された[9]．1995年にはIshakらによって新しいHAIスコアの分類法が報告され，炎症はgradingで，線維化はstagingとして表現される方法が一般化した．この時点で，piecemeal necrosis（削り取り壊死）と呼ばれていた門脈周囲の肝細胞死の主体がアポトーシスであることが明らかになってきたため，interface hepatitisと表現されるようになっている．わが国でも，同様の時期に犬山分類の検討が行われ，1994年に新犬山分類として提案され，1996年に現在の基準が確定した[10]．

6　B型肝炎とC型肝炎—線維化の進展予測

B型慢性肝炎は，活動性の強い時期には炎症が強く，線維化も急速に進行することがあるが，一方で，HBe抗原のseroconversionを起こしたあとでは炎症は消失し，その後の線維化進展がほとんどみられない症例も多い．このようにB型肝炎では病勢の変動が大きいため，線維化は一定の速度では進展せず，長期的な予後を推測することは容易ではない．

C型慢性肝炎の場合にも，線維化進展には

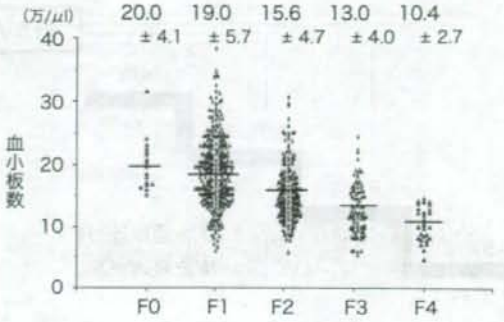

図1　Fスコアと血小板数

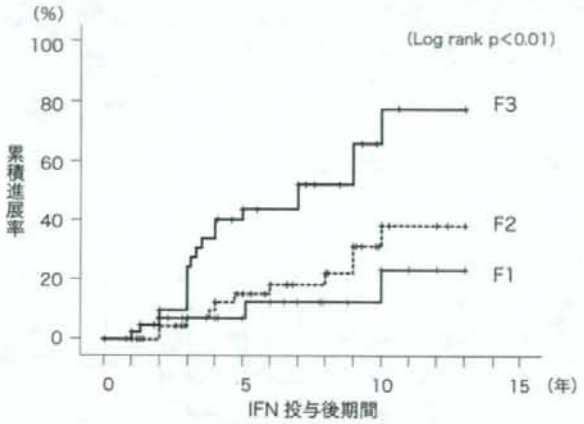

図2　肝線維化と肝硬変への進展

個人差があるが，C型肝炎症例全体としては，経過とともに進展する例が多い．Poynardら[11]は，感染時期が特定できる患者の肝生検結果から，線維化スコアの進展速度を年率0.133と報告した．また，Shiratoriら[12]は，同一患者への経時的な2回の肝生検から線維化スコアの進展速度を年率0.10と算出している．これらの結果からは，肝硬変までの進展が約30年であることを表しており，臨床的な成績ともほぼ合致する．なおC型肝炎例では，ALT持続正常例の線維化進展は緩徐で，一方，男性，アルコール多飲，高齢時感染などでは線維化進展は速い傾向にあると考えられている．

7　C型肝炎の線維化と血小板数

C型慢性肝炎では，線維化の進行と血小板数の減少が相関することが知られている．肝の線維化を非侵襲的に評価する方法としては，線維化マーカーやFibroscanによるものなどがあるが，血小板数は検査が簡単で，かつ臨床的な有用性が高く評価されている．

図1は，当科のC型慢性肝疾患患者の肝生検によるFスコア別の血小板数を示してい

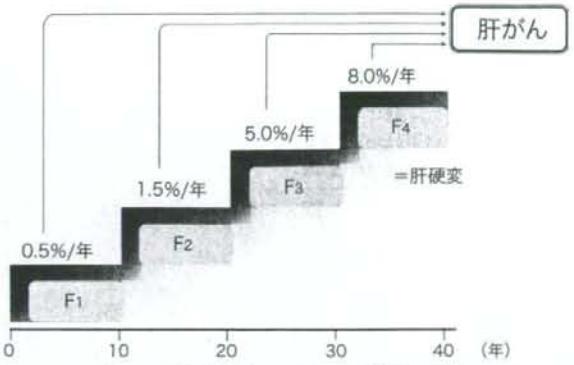

図3　C型慢性肝炎における肝線維化の進行

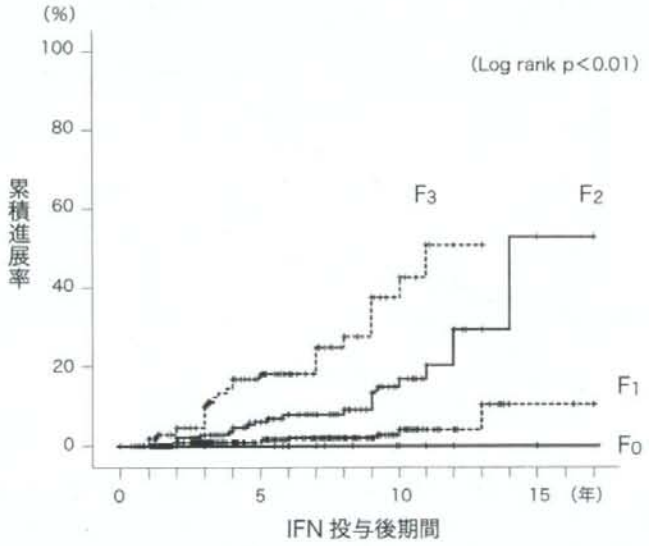

図4　IFN治療時の線維化の程度と肝硬変への進展

る．各スコアの平均血小板数(/μL)は，F0で20.0万，F1で19.0万，F2で15.6万，F3で13.0万，F4で10.4万であった．Fスコアが高値になるほど血小板数の平均値は減少傾向を示している．ただし，同一スコア内でも血小板数のばらつきが大きいことには注意が必要である．個々の症例では，線維化に関連する他の検査結果や，経時的な血小板数の変動も含めて，臨床的に判断することが望ましい．

8　C型肝炎の線維化進展

C型慢性肝炎の自然経過において線維化は経時的に進展し，年率で約3%の頻度で慢性肝炎から肝硬変へ進行する．無治療・自然経

表2　IFN治療効果別の肝硬変への進展例

	著効	再燃	無効	計
F_0	0/13 (0%)	0/8 (0%)	−	0/21 (0%)
F_1	0/191 (0%)	3/187 (0.2%)	3/35 (1.5%)	6/413 (0.2%)
F_2	0/87 (0%)	11/87 (1.8%)	11/59 (3.4%)	22/233 (1.6%)
F_3	0/38 (0%)	6/44 (2.5%)	20/47 (9.3%)	26/129 (4.0%)
計	0/329 (0%)	20/326 (0.9%)	34/141 (4.7%)	54/796 (1.2%)

(カッコ内は年率)

過観察例を対象とした解析では，病期進展例の頻度が実際より低率になる可能性が高いため，ここではインターフェロン治療例の内，無反応例を対象として肝硬変進展率を検討した．これらの対象では，治療を要すると判断される症例の無治療・自然経過に類似するものと考えられる．

対象は1990年代に，肝生検施行後，従来型のインターフェロン治療(6カ月以内)を施行したC型慢性肝疾患症例796例である．治療効果は，著効329例(41.3%)，再燃326例(41.0%)，無効141例(17.7%)であった．この無効例における，治療開始時のFスコアとそののちの肝硬変進展率をKaplan-Meier法で示す(図2)．インターフェロン治療開始後の5年後および10年後の肝硬変進展率は，F1例では6.9%，23.3%，F2例では14.9%，38.1%，F3例では43.5%，77.3%と，Fスコアが高い症例ほど，早期かつ高率に肝硬変への進展を示した．

同様にFスコアが高いほど，肝癌発生の可能性も高くなる．特に，F4の肝硬変と診断されたのちでは，肝癌発生のリスクも非常に高くなる(図3)．

9 C型肝炎に対するインターフェロン治療と肝線維化

肝の線維化は，インターフェロン治療効果にも関連し，線維化が進行するほど，難治傾向を示す．前述のインターフェロン治療症例全体を対象として，インターフェロン治療を行ったのちの経過観察における肝硬変への進展度をFスコア別に表す(図4)．この解析は著効・再燃・無効のすべての例が対象であり，図2と比較すると，同じFスコアの症例でも，インターフェロン治療がそののちの予後を改善し，肝硬変への進展を抑制していることが示されている．この対象症例を，Fスコア別・治療効果別に分けて，治療後の肝硬変進展率を示す(表2)．Fスコア別の肝硬変進展に関する年率は，F0では0%，F1が0.2%，F3が1.6%，F3で4.0%であった．ウイルス学的著効例からの肝硬変進展は認めなかったが，再燃例あるいは無効例のそれぞれの対象に限定した場合も，線維化の程度と肝硬変進展率に相関がみられる．

また，Shiratoriら[12]の検討で，インターフェロン治療によりC型肝炎ウイルスが完全に排除された症例では，Fスコアが年率0.28の速度で低下することが明らかとなり，治療前の線維化進展速度よりも速く，線維化の改善が得られることが報告されている．このように肝の病態，あるいは治療効果評価をFスコアを用いて解析することにより，長期経過のなかでの肝疾患の予後の評価も客観化が可能となった．

10 おわりに

ウイルス性肝炎に伴う肝臓の線維化は，肝内の慢性的な炎症の繰り返しの結果，沈着が蓄積していく．したがって，肝線維化はウイルス性肝炎の「慢性度」を表し，スコア化して評価することは臨床的に有効である．ウイルス性肝炎に対する治療効果も，短期的なウイルス学的・生化学的有効性から評価するだけでなく，病期の進行あるいは発癌など，長期予後の観点からの評価の必要性が認識されるようになり，肝線維化はさらに重要な臨床的指標となってきた．

文　献

1) 中野雅行：肝線維化の形態学．肝臓病学　Basic Science，戸田剛太郎，織田正也，清澤研道，他編，医学書院，1998，pp670–678
2) Canbay A, Friedman S, Gores GJ : Apoptosis: The nexus of liver injury and fibrosis. Hepatology 39 : 273–278, 2004
3) Kage M, Shimamatu K, Nakashima E et al : Longterm evolution of fibrosis from chronic hepatitis to liver cirrhosis in patients with hepatitis C : Morphologic analysis of repeated biopsies. Hepatology 25 : 1028–1031, 1997
4) 鹿毛政義：新しい慢性肝炎分類 基本組織像と分類の実際．肝・胆・膵フロンティア1，慢性肝炎新分類のすべて．診断と治療社，1998，pp20–30
5) Knodell RG, Ishak KG, Black WC et al : Formulation and application of a numerical scoring system for assessing histological activity in asymptomatic chronic active hepatitis. Hepatology 1 : 431–435, 1981
6) Brunt EM : Grading and staging the histopathological lesions of chronic hepatitis : The Knodell histology activity index and beyond. Hepatology 31 : 241–246, 2000
7) Scheuer PJ : Classification of chronic viral hepatitis; a need for reassessment. J Hepatol 13 : 372–374, 1991
8) Desmet VJ, Gerber M, Hoofnagle JH et al : Classification of chronic hepatitis : diagnosis, grading and staging. Hepatology 19 : 1513–1520, 1994
9) French METAVIR Cooperative Study Group : Intraobserver and interobserver variations in liver biopsies in patients with chronic hepatitis C. Hepatology 20 : 15–20, 1994
10) Ichida F, Tsuji T, Omata M et al : New Inuyama classification; new criteria for histological assessment of chronic hepatitis. International Hepatol Com 6 : 112–119, 1996
11) Poynard T, Bedossa P, Opolon P et al : Natural history of liver fibrosis progression in patients with chronic hepatitis C. Lancet 349 : 825–832, 1997
12) Shiratori Y, Imazeki F, Moriyama M et al : Histologic improvement of fibrosis in patients with hepatitis C who have sustained response to interferon therapy. Ann Intern Med 132 : 517–524, 2000

*　　*　　*

Available online at www.sciencedirect.com
SCIENCE DIRECT
ELSEVIER
Hepatology Research 35 (2006) 135–139
HEPATOLOGY RESEARCH
http://www.elsevier.com/locate/hepres

Usefulness of elastometry in evaluating the extents of liver fibrosis in hemophiliacs coinfected with hepatitis C virus and human immunodeficiency virus

Naohiko Masaki [a,*], Masatoshi Imamura [a], Yoshimi Kikuchi [b], Shinichi Oka [b]

[a] *Division of Gastroenterology, International Medical Center of Japan, Toyama 1-21-1, Shinjuku-ku, Tokyo 162-8655, Japan*
[b] *Division of AIDS Research Center, International Medical Center of Japan, Tokyo 162-8655, Japan*

Received 31 October 2005; received in revised form 13 February 2006; accepted 15 February 2006

Abstract

The newly developed elastometer, FibroScan®, was utilized to evaluate liver fibrosis in hepatitis C virus (HCV)- and human immunodeficiency virus (HIV)-coinfected 33 hemophiliacs and HIV-uninfected 24 patients with chronic hepatitis C. Chronicity in the liver was categorized into 4 stages by abdominal ultrasound (AUS): 1 (normal or fatty liver); 2 (chronic liver disease, mild); 3 (moderate); and 4 (severe). Stiffness of the liver was significantly increased as AUS stages advanced: 5.4 ± 2.2 ($N=3$) versus 7.5 ± 2.7 ($N=9$), in stage 1; 4.9 ± 1.7 ($N=2$) versus 9.9 ± 6.0 ($N=10$), in stage 2, 13.5 ± 4.7 ($N=5$) versus 12.9 ± 5.9 ($N=6$), in stage 3, and 22.0 ± 9.5 ($N=14$) versus 28.1 ± 21.3 ($N=8$), in stage 4, in non-HIV group and in HIV group, respectively ($P=0.004$ and 0.007). Stiffness was correlated with AUS stages ($r=0.740$, $P<0.001$), platelet counts (PLT; $r=-0.642$, $P=0.001$) and 7S domain of type IV collagen (IV-coll; $r=0.480$, $P=0.024$) in non-HIV group, while in HIV group, with IV-coll ($r=0.801$, $P<0.001$), AUS stages ($r=-0.603$, $P<0.001$), procollagen type III peptides (P-III-P; $r=0.621$, $P=0.001$), PLT ($r=-0.480$, $P=0.005$), and hyaluronic acid ($r=0.433$, $P=0.027$). FibroScan® is absolutely noninvasive and can be the alternative to liver biopsy, especially in patients with bleeding tendency.

Keywords: Liver fibrosis; HCV; HIV; Stiffness

1. Introduction

It has been well documented that coinfection of hepatitis C virus (HCV) and human immunodeficiency virus (HIV) might accelerate the progression of liver fibrosis, as compared with HCV infection alone [1]. However, especially in patients with hemophilia coinfected with HCV and HIV, it is practically difficult to perform liver biopsy, the established gold standard to evaluate the extents of liver fibrosis, because of their bleeding tendency. Moreover, tiny biopsied specimens, corresponding to only one forty thousandth of entire liver volume, may sometimes cause misleading explanations. Although rough estimation of liver fibrosis can be performed by abdominal ultrasound (AUS), it would be somewhat subjective and dependent on technical experience. In addition, several serum markers for liver fibrosis such as procollagen type III peptides (P-III-P), 7S domain of type IV collagen (IV-coll), and hyaluronic acid, have been commercially available, however, those substances might just reflect overproduction of collagen in vivo.

Recently, a new noninvasive device to quantify liver fibrosis, FibroScan®, was developed by Echosens (Paris, France). This device is based on one-dimensional transient elastography, using both ultrasound (5 MHz) and low-frequency (50 Hz) elastic waves, whose propagation velocity is directly proportional to elasticity [2]. Usefulness of this device to assess the extents of liver fibrosis in patients with chronic hepatitis was already reported from France [3], and from Japan [4]. In this study, we attempted to evaluate its usefulness

* Corresponding author. Tel.: +81 3 3202 7181; fax: +81 3 3207 1038.
E-mail address: nmasaki@imcj.hosp.go.jp (N. Masaki).

1386-6346/$ – see front matter © 2006 Elsevier Ireland Ltd. All rights reserved.
doi:10.1016/j.hepres.2006.02.006

in hemophiliacs coinfected with HCV and HIV, in whom liver biopsy is ordinarily contraindicated, as well as in non-hemophiliacs infected by HCV alone.

2. Patients and methods

Hemophiliacs coinfected with HCV and HIV or non-hemophiliacs infected by HCV alone, who consulted Division of AIDS Research Center or Division of Gastroenterology, International Medical Center of Japan, from February to April, 2004, were randomly enrolled in this study, after informed consent was given. The patient received elastometry with FibroScan® version 2 (FibroScan® 502: Echosens, Paris, France), as previously reported [4], at the same time with B-mode AUS, by two hepatologists (N.M. and M.I.) with over 15-year experience. The elasticity of the liver was measured 10 times and the median value, which was automatically calculated, was considered as Stiffness (KPa). AUS findings of the liver were categorized into 4 stages, based on the extents of surface irregularity, dullness of the edge, heterogeneity of internal echogenecity, blurriness of hepatic veins, and imbalance in size of both lobes (hypertrophy of the caudate lobe and/or atrophy of the right lobe): (1) normal or fatty liver; (2) chronic liver disease, mild; (3) moderate; and (4) severe. On the same day, serum levels of albumin, alanine aminotransferase (ALT), and liver fibrosis markers (P-III-P, IV-coll, and hyaluronic acid), were measured. HCV genotype and peripheral platelet counts (PLT) were also determined. Only in HIV group, CD4 counts and HIV RNA concentrations were determined. The correlation between Stiffness and AUS stage, PLT, or serum liver fibrosis markers were investigated.

In patients, where the age of blood transfusion or the first infusion of clotting factor concentrates could be identified, annual progression rate of liver fibrosis (R-value: KPa/year) was arbitrarily calculated, according to the following equation. R-value = [Stiffness − 5.4]/[Age (at the elastometry) − Age (of the HCV infection)], where 5.4 is the mean value of Stiffness in patients with normal AUS finding (data shown in Section 3).

2.1. Statistical analysis

The data were shown as mean ± standard deviation. The correlation between the Stiffness and AUS stage was determined by Kruskal–Wallis test. The correlation between the parameters was determined by Pearson's correlation coefficient or Spearman's correlation coefficient. The comparisons between the data were analyzed by Mann–Whitney U-test or Fisher's exact test.

3. Results

Thirty-three hemophiliacs coinfected with HCV and HIV (HIV group; hemophilia A/B = 23 patients/10 patients; all males) and 24 non-hemophiliacs infected by HCV alone (non-HIV group; 12 males and 12 females), were enrolled in this study, and received B-mode AUS and elastmetry at the same time. The demographic features and laboratory data of both groups were shown in Table 1. All the patients in HIV group have been successfully treated by highly active antiretroviral therapy (HAART) since 1996, and in 23 patients, HIV RNA concentrations were maintained less than 50 copy/ml. Seven out of 21 (33%) patients in HIV group were infected by HCV with uncommon genotype in Japan (1a or 3a). The patients were classified into 4 stages on AUS: stage 1: 3 and 9; stage 2: 2 and 10; stage 3: 5 and 6; stage 4: 14 and 8, in non-HIV group and HIV group, respectively. Apparently, in non-HIV group, most of the patients were older and had more advanced stages of chronic liver disease, as compared with those in HIV group. Stiffness of the liver in each AUS stage was shown as follows: 5.4 ± 2.2 and 7.5 ± 2.7, in stage 1; 4.9 ± 1.7 and 9.9 ± 6.0, in stage 2, 13.5 ± 4.7 and 12.9 ± 5.9, in stage 3, 22.0 ± 9.5 and 28.1 ± 21.3, in stage 4,

Table 1
Demographic features and laboratory data of non-HIV group and HIV group

Parameters	Non-HIV group (N = 24)	HIV group (N = 33)	P-value
Age	69 ± 13	39 ± 11	0.000[a]
Gender (M/F)	12/12	33/0	0.000[b]
Albumin (g/dl)	4.0 ± 0.4	4.3 ± 0.3	0.004[a]
ALT (U/l)	60 ± 45	67 ± 54	NS[a]
PLT ($\times 10^4/\mu l$)	12.5 ± 5.2	19.0 ± 8.6	0.003[a]
CD4 counts (μl^{-1})	n.d.	442 ± 230	
P-III-P (U/ml)	1.2 ± 0.3	0.9 ± 0.3	0.003[a]
IV-coll (ng/ml)	8.3 ± 3.1	6.2 ± 2.7	0.013[a]
Hyaluronic acid (ng/ml)	335 ± 399	210 ± 190	NS[a]
HCV genotype (1/1a/1a + 1b/1b/2a/2b/3a/3a + 2b)	2/0/0/8/1/2/0/0	4/4/1/5/3/2/1/1	
AUS stage (1/2/3/4)	3/2/5/14	9/10/6/8	0.031[c]

n.d.: not determined, NS: not significant. The abbreviations used are: ALT, alanine aminotransferase; PLT, platelet counts; P-III-P, procollagen type III peptides; IV-coll, 7S domain of type IV collagen; AUS, abdominal ultrasound.

[a] Mann–Whitney U-test.

[b] Fisher's exact test.

[c] Pearson's χ^2-test.

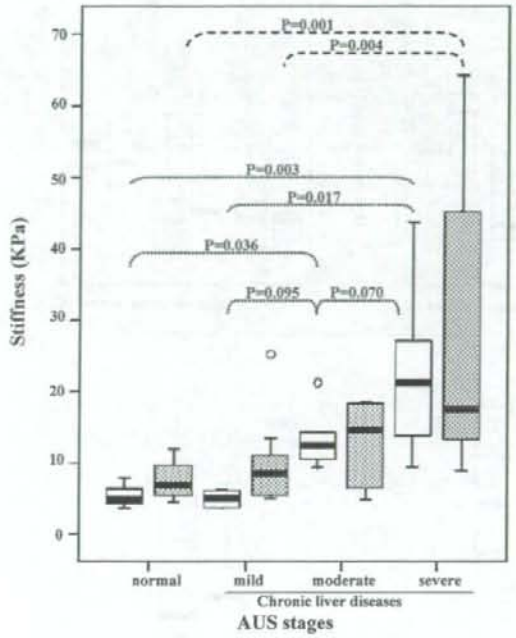

Fig. 1. Box plots of Stiffness for each AUS stage in non-HIV group and HIV group. The *top* and *bottom* of the boxes are the first and third quartiles, respectively. The length of the box represents the interquartile range within which 50% of the values were located. The *line* through the middle of each box represents the median. The *error bars* show the minimum and maximum values. Open boxes and dotted boxes show the data of non-HIV group and those of HIV group, respectively. The *P*-value was calculated by Mann–Whitney *U*-test.

in non-HIV group and in HIV group, respectively ($P=0.004$ and 0.007, by Kruskal–Wallis test in each group). There was no significant difference between non-HIV group and HIV group, in each AUS stage. Box plots of Stiffness for each AUS stage were demonstrated in Fig. 1. In non-HIV group, there existed significant difference in Stiffness between stages 4 and 2 ($P=0.017$), between stages 4 and 1 ($P=0.003$), and between stages 3 and 1 ($P=0.036$). In addition, there was marginal difference between stages 4 and 3 ($P=0.070$), and between stages 3 and 2 ($P=0.095$). While, in HIV group, Stiffness in stage 4 was significantly higher than that in stage 1 ($P=0.001$), and that in stage 2 ($P=0.004$).

To examine usefulness of elastometry in differentiating advanced stage of chronic liver disease from non-advanced one, similar analysis was conducted after patients of stages 2 and 3 were combined together. Chronicity in the liver was simply categorized into 3 modified AUS stages: normal (stage 1), non-advanced (stage 2+3) and advanced (stage 4). Stiffness of the liver in each modified AUS stage was shown as follows: 5.4 ± 2.2 ($N=3$) and 7.5 ± 2.7 ($N=9$), in stage 1 (normal), 11.1 ± 5.7 ($N=7$) and 11.1 ± 6.0 ($N=16$), in stage 2+3 (non-advanced), 22.0 ± 9.5 ($N=14$) and 28.1 ± 21.3 ($N=8$), in stage 4 (advanced), in non-HIV group and in HIV group, respectively ($P=0.003$ and 0.004, by Kruskal–Wallis test in each group). Again, there was no significant difference between non-HIV group and HIV group, in each modified AUS stage. In addition, as compared with other liver fibrosis markers such as P-III-P, IV-coll, hyaluronic acid, and PLT, Stiffness was found to be the most useful in differentiating advanced stage of chronic liver disease from non-advanced one, both in non-HIV group and in HIV group (Fig. 2).

3.1. Correlation between Stiffness and other parameters for liver fibrosis

To evaluate usefulness of elastometry, we investigated correlation between Stiffness and conventional liver fibrosis markers such as P-III-P, IV-coll, and hyaluronic acid, including AUS stage and PLT. In non-HIV group, Stiffness was significantly correlated with AUS stage ($r=0.740$, $P<0.001$), PLT ($r=-0.642$, $P=0.001$), and IV-coll ($r=0.480$, $P=0.024$). On the other hand, in HIV group, Stiffness was significantly correlated with IV-coll ($r=0.801$, $P<0.001$), AUS stage ($r=0.603$, $P<0.001$), P-III-P ($r=0.621$, $P=0.001$), PLT ($r=-0.480$, $P=0.005$), and hyaluronic acid ($r=0.433$, $P=0.027$).

3.2. Correlation between platelet counts and other parameters for liver fibrosis

It has been well established that PLT are inversely proportional to the extents of liver fibrosis [5]. In this study, we investigated correlation between PLT and conventional liver fibrosis markers, AUS stage or Stiffness. In non-HIV group, PLT were significantly correlated with AUS stage ($r=-0.647$, $P=0.001$), IV-coll ($r=-0.643$, $P=0.001$), Stiffness ($r=-0.642$, $P=0.001$), P-III-P ($r=-0.526$, $P=0.012$), and hyaluronic acid ($r=-0.424$, $P=0.049$). On the other hand, in HIV group, PLT were significantly correlated with Stiffness ($r=-0.480$, $P=0.005$), AUS stage ($r=-0.415$, $P=0.016$), and IV-coll ($r=-0.417$, $P=0.031$).

3.3. Annual progression rate of liver fibrosis

We attempted to evaluate whether HIV coinfection may affect progression of liver fibrosis in patients with chronic hepatitis C. In non-HIV group, the age of blood transfusion was identified in 9 patients. Two of them had received interferon (IFN) therapy: IFN monotherapy and IFN-α2b/ribavirin, each, without sustained virological response (SVR). On the other hand, in HIV group, they had received multiple infusions of clotting factor concentrates, it was practically impossible to determine the time of the first infection of HIV or HCV. We speculated the age of the first infusion of such concentrates as the time of HCV infection, in 23 patients, in order to arbitrarily calculate annual progression rate of liver fibrosis (*R*-value). Twelve out of them had history of IFN therapy: IFN monotherapy, IFN-α2b/ribavirin and Pegylated IFN-α2a in 3, 5 and 4 patients,

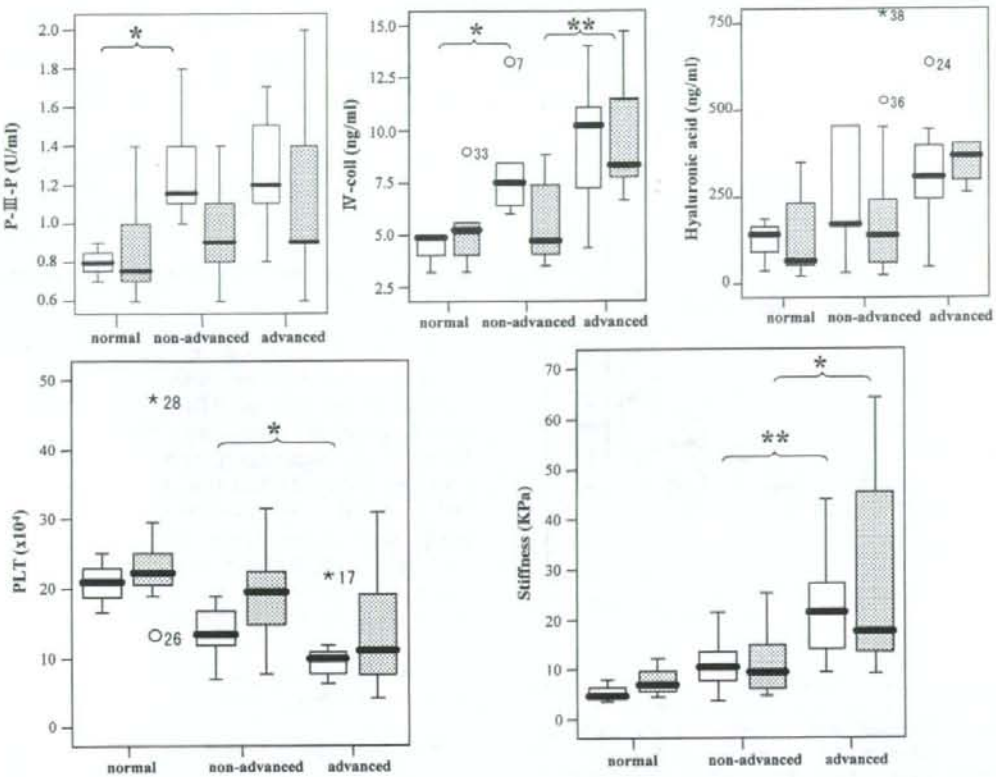

Fig. 2. Box plots of liver fibrosis markers (P-III-P, IV-coll, hyaluronic acid), PLT and Stiffness for each modified AUS stage in non-HIV group and HIV group. Open boxes and dotted boxes show the data of non-HIV group and those of HIV group, respectively. The P-value was calculated by Mann–Whitney U-test ($^{*}P<0.05$, $^{**}P<0.01$).

respectively. Four of them (33%) obtained SVR. There was no significant difference in R-value between non-HIV group and HIV group (0.32 ± 0.17 versus 0.38 ± 0.70; $P = 0.125$, by Mann–Whitney U-test). In HIV group, there was no significant difference in R-value between IFN-treated ($N = 12$) and untreated ($N = 11$) patients (0.34 ± 0.50 versus 0.43 ± 0.90, $P = 0.710$). Furthermore, in HIV group treated by IFN, there was no significant difference in R-value between patients with SVR ($N = 4$, 0.08 ± 0.10) and those without SVR ($N = 7$, 0.52 ± 0.60; $P = 0.252$).

4. Discussion

In this study, we attempted to validate Stiffness measured by the newly developed elastometer, FibroScan® 502, in evaluating the extents of liver fibrosis in hemophiliacs coinfected with HIV and HCV (HIV group). Non-hemophiliacs infected by HCV alone (non-HIV group), could be regarded as a control, since hemophilia per se may not affect inflammation or fibrosis in the liver. It has been recently established that Stiffness is strongly correlated with liver fibrosis markers as well as F score evaluated by liver biopsy, in non-HIV group [3,4]. Liver biopsy could not be practically performed in clinical settings, however, such correlation was similarly, and even more significantly, confirmed also in HIV group. In this study, correlation between Stiffness and other parameters for liver fibrosis was rather weak in non-HIV group where more than half of the patients might have liver cirrhosis, probably because the variations of such liver fibrosis markers were greater in more advanced stage of chronic liver disease as shown in Fig. 2, as well as described previously [4]. Although AUS findings might be somewhat subjective, Stiffness in stage 4 was significantly higher than those in stages 1 and 2, both in HIV group and in non-HIV group, in this study (Fig. 1). In addition, when the patients of stages 2 and 3 were combined together, Stiffness was the only tool in differentiating advanced stage of chronic liver disease from non-advanced one, both in non-HIV group and in HIV group, as shown in Fig. 2. Accordingly, measurement of Stiffness could be a very useful tool to identify patients, at least, with advanced liver fibrosis. In contrast, PLT, which have been widely accepted as one of the very sensitive markers for liver fibrosis [5], seemed to be less reliable in HIV group than in

non-HIV group. Possibility of influence of HAART regimens on PLT counts should be further investigated in a future study.

It has been occasionally described that HIV coinfection increases the risk of cirrhosis and even hepatocellular carcinoma (HCC) in HCV-infected patients [6]. In addition, whether introduction of HAART or IFN therapy could affect these situations would be undoubtedly our major concern. Kramer et al. [7] recently reported that HIV coinfection accelerated liver fibrosis in pre-HAART era, but not in HAART era, while it did not affect the risk of HCC in HCV infected U.S. veterans in both eras. Similarly, Marine-Barjoan et al. [8] found that early HAART may slow liver fibrosis progression in coinfected French patients. On the contrary, Martinez-Sierra et al. [9] showed that the immune response to HAART did not influence liver fibrosis progression rate in coinfected Spanish patients. Moreover, it has been recently pointed out that HAART regimens including nevirapine, one of nonnucleoside reverse-transcriptase inhibitors, may be associated with faster liver fibrosis progression in coinfected patients [10], especially with advanced stages of liver fibrosis [11]. In this study, we arbitrarily calculated annual progression rate of liver fibrosis, using Stiffness and duration of HCV infection. Interestingly, there was no significant difference between non-HIV group and HIV group receiving HAART. This may be quite consistent with our previous findings that plasma levels of TGF-β and IL-13, known cytokines to play pivotal roles in liver fibrosis, were significantly decreased in coinfected patients under HAART, as compared with those in patients infected HCV alone (unpublished results). Furthermore, we could not get any definitive results that IFN therapy may counteract progression of liver fibrosis, because of the small numbers of patients examined and short terms of follow-up after IFN therapy. Further regular check-ups of the elasticity of the liver would be prerequisite to settle these controversial issues.

In conclusion, FibroScan® is absolutely noninvasive and can be the alternative to liver biopsy, especially in patients with bleeding tendency. It is strongly suggested that HIV/HCV coinfection may not accelerate liver fibrosis progression in HCV-related chronic liver disease, at least in HAART era.

Acknowledgements

This work was supported by Grant-in-Aid for Health Sciences Research Grants of The Ministry of Health, Welfare and Labor, Japan.

References

[1] Di Martino V, Rufat P, Boyer N, et al. The influence of human immunodeficiency virus coinfection on chronic hepatitis C in injection drug users: a long-term retrospective cohort study. Hepatology 2001;34:1193–9.
[2] Sandrin L, Fourquet B, Hasquenoph JM, et al. Transient elastography: a new noninvasive method for assessment of hepatic fibrosis. Ultrasound Med Biol 2003;29:1705–13.
[3] Castera L, Vergniol J, Foucher J, et al. Prospective comparison of transient elastography, Fibrotest, APRI, and liver biopsy for the assessment of fibrosis in chronic hepatitis C. Gastroenterology 2005;128:343–50.
[4] Saito H, Tada S, Nakamoto N, et al. Efficacy of non-invasive elastometry on staging of hepatic fibrosis. Hepatol Res 2004;29:97–103.
[5] Adinolfi LE, Giordano MG, Andreana A, et al. Hepatic fibrosis plays a central role in the pathogenesis of thrombocytopenia in patients with chronic viral hepatitis. Br J Haematol 2001;113:590–5.
[6] Darby SC, Ewart DW, Giangrande PL, et al. Mortality from liver cancer and liver disease in haemophiliac men and boys in UK given blood products contaminated with hepatitis C. UK Haemophilia Centre Directors' Organisation. Lancet 1997;350:1425–31.
[7] Kramer JR, Giordano TP, Souchek J, et al. The effect of HIV coinfection on the risk of cirrhosis and hepatocellular carcinoma in U.S. veterans with hepatitis C. Am J Gastroenterol 2005;100:56–63.
[8] Marine-Barjoan E, Saint-Paul MC, Pradier C, et al. Impact of antiretroviral treatment on progression of hepatic fibrosis in HIV/hepatitis C virus co-infected patients. AIDS 2004;18:2163–70.
[9] Martinez-Sierra C, Arizcorreta A, Diaz F, et al. Progression of chronic hepatitis C to liver fibrosis and cirrhosis in patients coinfected with hepatitis C virus and human immunodeficiency virus. Clin Infect Dis 2003;36:491–8.
[10] Macias J, Castellano V, Merchante N, et al. Effect of anriretroviral drugs on liver fibrosis in HIV-infected patients with chronic hepatitis C: harmful impact of nevirapine. AIDS 2004;18:767–74.
[11] Aranzabal L, Casado JL, Moya J, et al. Influence of liver fibrosis on highly active antiretroviral therapy-associated hepatotoxicity in patients with HIV and hepatitis C virus coinfection. Clin Infect Dis 2005;40:588–93.

Virology 379 (2008) 306–313

Contents lists available at ScienceDirect

Virology

journal homepage: www.elsevier.com/locate/yviro

Human T-cell leukemia virus type 1 Tax modulates interferon-α signal transduction through competitive usage of the coactivator CBP/p300

Jing Zhang [a,*], Osamu Yamada [a], Kenji Kawagishi [a], Hiromasa Araki [a], Shoji Yamaoka [b], Toshio Hattori [c], Kunitada Shimotohno [d,e]

[a] Research and Development Center, FUSO Pharmaceutical Industries, LTD., 2-3-30 Morinomiya, Joto-ku, Osaka 536-8523, Japan
[b] Department of Molecular Virology, Graduate School of Medicine, Tokyo Medical and Dental University, Tokyo, Japan
[c] Department of Infectious and Respiratory Diseases, Tohoku University School of Medicine, Sendai, Japan
[d] Center for Integrated Medical Research, Keio University School of Medicine, Tokyo, Japan
[e] Research Center, Chiba Institute of Technology, Chiba, Japan

ARTICLE INFO

Article history:
Received 2 May 2008
Returned to author for revision 18 June 2008
Accepted 30 June 2008
Available online 3 August 2008

Keywords:
HTLV-1
Tax
IFN-α signaling
CBP/p300 coactivator

ABSTRACT

We describe here Tax protein of human T-cell leukemia virus type 1 (HTLV-1) as an interferon (IFN)-α antagonist counteracting the transactivation function of IFN-stimulated gene factor 3 (ISGF3). Co-expression of Tax, but not the Tax mutant unable to bind to CBP, significantly inhibited the reporter gene expression directed by IFN-stimulated regulatory elements, despite that the formation of DNA-binding ISGF3 complex was unaffected. Gene activation induced by STAT2 transcription domain was also inhibited by expression of Tax. Furthermore, Tax-mediated transcriptional inhibition was reversed by overexpression of p300. These observations indicate that Tax interferes with IFN-α-induced JAK-STAT pathway by competition with STAT2 for CBP/p300 binding. Consistently, GST pull-down assay showed that Tax dose-dependently inhibited binding of STAT2 to p300. This study suggests that Tax may prevent IFN-α from exerting its antiviral, antiproliferative and proapoptotic effects, thereby contributing to persistent viral infection and HTLV-1-associated oncogenesis.

Introduction

Human T-cell leukemia virus type 1 (HTLV-1) is an oncogenic retrovirus responsible for development of adult T-cell leukemia/lymphoma (ATLL) (Yoshida et al., 1984) and HTLV-1-associated neurodegenerative diseases such as myelopathy/tropical spastic paraparesis (HAM-TSP) (Gessain et al., 1985; Osame et al., 1986). ATLL is highly chemoresistant and its prognosis is usually poor. After conventional chemotherapy failure, interferon (IFN)-α combined with antiretroviral reagents such as zidovudine produces clinical remission followed by progression and death (Gill et al., 1995; Hermine et al., 1995). HTLV-1-associated oncogenesis has been demonstrated to be largely attributable to the expression of the viral regulatory protein Tax (Grassmann et al., 1989; Grassmann et al., 1992). In addition to its role in activating proviral transcription, Tax has been shown to activate transcription through protein–protein interactions with multiple transcription factors including the cyclic AMP-responsive element-binding factor (CREB), NF-κB, and the serum-responsive element-binding factor (SRF). Tax stimulates viral transcription through interacting with three conserved 21-bp repeat DNA elements known as viral CREs located within the HTLV-1 promoter. Tax binds to the CRE sequences in complex with the transcriptional factor CREB, which subsequently facilitates the transcription by recruitment of the cellular coactivators CBP (CREB-binding protein) and p300 (Giebler et al., 1997; Kwok et al., 1996).

CBP and p300 were originally identified as targets of CREB and adenovirus E1A, respectively (Chrivia et al., 1993; Eckner et al., 1994). They are large nuclear phosphoproteins that act as global transcriptional coactivators by binding numerous transcription factors (Janknecht and Hunter, 1996). CBP/p300 functions as coactivator or adapter by bridging transcription factors to general transcription machinery such as TFIIB, TBP and RNA polymerase II. In addition, CBP/p300 might contribute to transcriptional regulation by acetylation of chromatin via its intrinsic histone acetyltransferase (HAT) activity or its association with another HAT, p/CAF (Bannister and Kouzarides, 1996; Ogryzko et al., 1996; Yang et al., 1996). The simultaneous interaction of multiple transcription factors with CBP/p300 has been proposed to contribute to transcriptional synergy. Conversely, competition for limiting amounts of CBP/p300 has been suggested as a potential mechanism for transcriptional repression.

IFNs are a family of immunomodulatory cytokines that are produced in response to virus infection and possess both antiviral and antiproliferative functions. Secreted IFNs act in an autocrine or paracrine fashion to activate JAK-STAT pathway by binding to IFN receptors (IFN-α/β to IFNAR1/IFNAR2 and IFN-γ to IFNGR1/IFNGR2).

* Corresponding author. Fax: +81 6 6964 2706.
E-mail address: j-zhang@fuso-pharm.co.jp (J. Zhang).

0042-6822/$ – see front matter © 2008 Elsevier Inc. All rights reserved.
doi:10.1016/j.virol.2008.06.035

The activated (phosphorylated) STAT proteins form homodimers, or heterodimers, with other STAT proteins, which subsequently translocate to nucleus and bind specific DNA sequences within the promoter region of IFN-stimulated genes (ISGs). In the case of signaling via IFN-α/β, heterodimer of phosphorylated STAT1 and STAT2 interacts with IFN regulatory factor 9 (IRF9; p48) to form the trimer transcription complex ISGF3 (IFN-stimulated gene factor 3). By recruiting the transcriptional coactivator CBP/p300, ISGF3 triggers the expression of a variety of genes driven by the promoter containing IFN stimulated response elements (ISRE). Viruses have evolved different strategies to subvert IFN response, mainly by interfering IFN induction, perturbing IFN signaling and inhibiting IFN-induced effectors. Viral proteins acting as IFN antagonists have been identified in a numbers of viruses belonging to different families. Additionally, employing its antiproliferative and proapoptotic properties, IFN has been used as a therapeutic agent for multiple hematological and non-hematological malignancies. The anti-tumor efficacy, however, is limited by emergence of IFN resistance, a phenomenon attributable to the functional defects involved in IFN signaling pathway (Sun et al., 1998).

Here we present evidence demonstrating that HTLV-1 Tax interferes with the JAK-STAT signal transduction pathway in response to IFN-α, and the mechanism underlying the antagonistic function involves interaction of Tax with coactivator CBP/p300 in competition with STAT2, thereby inhibiting the transcription activation of STAT2-containing ISGF3 complex.

Results

Inhibition of IFN-α-induced ISRE signaling by Tax

By analyzing the influence of Tax protein on replication of hepatitis C virus (HCV) replicon, we previously showed an attenuated IFN-α-induced antiviral response in Tax-expressing Huh-7 cells (Zhang et al., 2007). If Tax inhibits IFN-α response, interference could occur via global interruption of the JAK-STAT signal transduction pathway or via inhibition of specific ISG products such as protein kinase R or 2′,5′-oligoadenylate synthetase. To define a possible role of Tax in modulating IFN-α signaling, Tax- or Tax mutant-expressing plasmid was transfected into Huh-7 cells together with the reporter vector pISRE-luc to monitor ISRE-directed gene expression. Cells were either left untreated or treated with 100 IU/ml of human IFN-α 24 h later, and the luciferase activity was measured following a further incubation for 24 h. As shown in Fig. 1A, both the wild type and the Tax mutant m148, previously demonstrated to be functional in activating CREB pathway while failing to activate NF-κB pathway, significantly inhibited IFN-α induced ISRE-directed luciferase expression, while the Tax mutant m319, unable to activate CREB pathway although retaining the ability to activate NF-κB pathway (Yamaoka et al., 1996), had no significant effect on ISRE-driven gene expression, indicating that Tax inhibits ISRE-directed gene expression and its competence for signaling through CREB is important for the observed inhibition. Western blot analysis showed a comparable expression of Tax and Tax mutants (Fig. 1B). Similar results were also observed with Jurkat T cells (Fig. 1C), suggesting that Tax-mediated inhibition of JAK-STAT signaling in response to IFN-α was not cell-type specific. These results suggest that Tax interferes with IFN-α response by a global transcriptional repression of downstream effector gene expression.

Tax does not affect the formation of DNA-binding ISGF3 complex

As forementioned above, IFN-α signaling through the JAK-STAT pathway involves a series of events including tyrosine phosphorylation of STAT1 and STAT2, formation and nuclear translocation of ISGF3 followed by its binding to ISREs. Impairment at any of these steps might consequently lead to blockade of IFN-α-induced signaling. To understand the mechanism employed by Tax to counteract IFN's

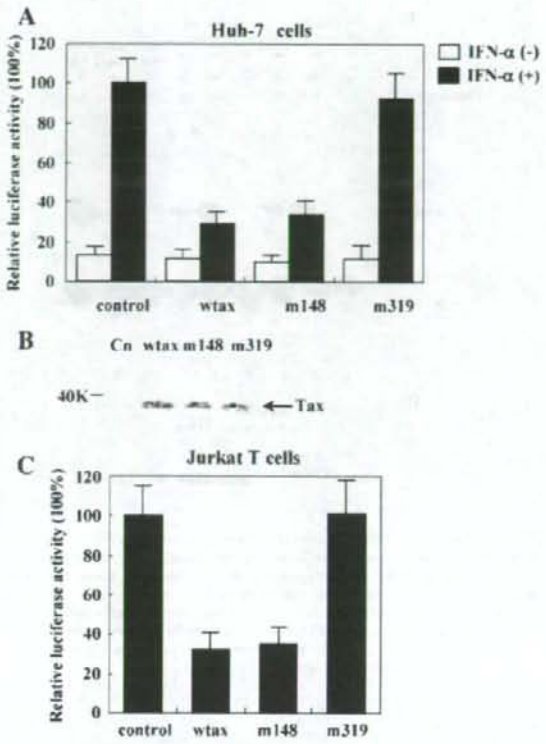

Fig. 1. Effect of Tax or its mutants on IFN-α-induced ISRE signaling. Huh-7 (A) or Jurkat T cells (C) were transfected with ISRE-luc together with pCn, pCnwtax, pCnm148, or pCnm319. Cells were either left untreated or treated with 100 IU/ml of human IFN-α 24 h later, and the luciferase activity was measured following a further incubation for 24 h. Renilla luciferase activities from cotransfected pRL-TK were used to normalize the transfection efficiency. Normalized luciferase activity from an otherwise identical control transfection with pCn backbone vector was set as 100%, and those in other transfectants are expressed as relative percentage. Results are presented as the means and standard deviations of four independent triplicate transfections. (B) Expression of Tax protein in each transfectant was confirmed by Western blot analysis. Solid arrow indicates the signals of Tax protein.

actions, we next investigated the formation of ISRE-binding ISGF3 in Huhwtax. Huhwtax is a cell line stably expressing Tax at a level comparable to HTLV-1-infected MT-2 cells (Fig. 2B), which was established by transfection with pCnwtax followed by G418 selection and limiting dilution (Zhang et al., 2007). Nuclear extracts were prepared and subjected to electrophoretic mobility shift assay (EMSA) using the labeled ISRE as an oligonucleotide probe. As seen in Fig. 2A, in IFN-α-treated HuhCn cells, which were stably transfected with the empty vector pCn and served as a negative control, ISRE–protein complexes of delayed electrophoretic mobility was detected (lane 2), which was diminished by addition of antibody against STAT1 or STAT2 (lanes 7–8) but not by irrelevant antibody to β-actin (lane 9), confirming the identity of the ISRE-binding factor as ISGF3. The formation of ISRE–protein complex was significantly inhibited by addition an excess of unlabeled ISRE as a competitor (lane 3), revealing the specificity of the observed ISRE–protein binding. Unexpectedly, IFN-α-induced ISGF3 formation in Huhwtax was comparable to that detected in HuhCn (lanes 4–6). While expression of Tax conferred an attenuated IFN-α-induced antiviral response in Huhwtax cells (Zhang et al., 2007), the formation of ISRE-binding ISGF3 complex in their nuclear extract was not affected, which suggests that Tax inhibits IFN-

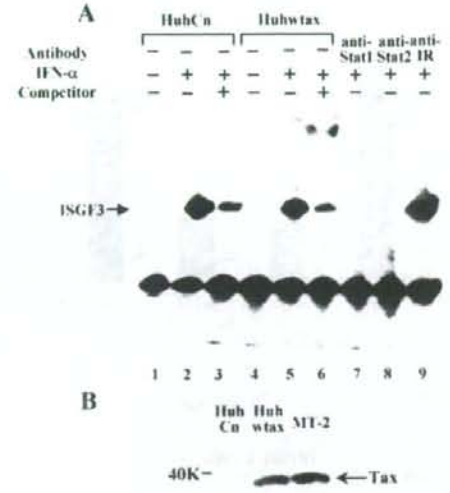

Fig. 2. Tax does not affect the formation of ISGF3 complex on ISRE promoter. (A) HuhCn or Huhwtax cells were treated in the absence or presence of 500 IU/ml of human IFN-α for 30 min. Nuclear extracts were prepared for EMSA analysis using labeled ISRE probe. In lanes 3 and 6, 50-fold molar excess of unlabeled ISRE competitor were included. In lanes 7–9, nuclear extracts were pre-incubated with the antibodies against STAT1, STAT2 or irrelevant β-actin (anti-IR) for 30 min prior to the addition of labeled probe. (B) Stable expression of Tax protein in Huhwtax cells was confirmed by Western blot analysis. Solid arrow indicates the signals of Tax protein.

α signaling without derailing the events involved in the formation of DNA-binding ISGF3 complex.

Tax represses transactivation function of STAT2

The results presented above imply that Tax averts IFN-α function via a mechanism other than inhibiting the activation and/or nuclear translocation of ISGF3 components. It is known that the C terminus of STAT2 serves as a transcriptional activation (TA) domain, which is essential for ISGF3 function. We next examined whether Tax could inhibit the transactivation function of STAT2. To this end, we constructed a vector pGAL4-Stat2(TA) by fusing the GAL4 DNA binding domain with the C-terminal 181 residues-coding region of STAT2. Expression of reporter gene from pGAL4-luc vector in HeLa cells was significantly induced by cotransfection with pGAL4-Stat2 (TA), but not by pGAL4-Stat2(TA)Δ with C-terminal 83 amino acids deleted, confirming the transactivation potential of the C terminus of STAT2 (Fig. 3). Importantly, cotransfection with Tax-expressing plasmid markedly inhibited the GAL4-Stat2(TA) transactivation activity, resulting in an approximately five- to six-fold lower luciferase expression when compared with the transfection in the absence of Tax. In contrast, the activation of the transcription from pGAL-luc by GAL4-VP16, which contains the activation domain of VP16 instead of Stat2 in GAL4-Stat2(TA), was not obviously affected by Tax protein, indicating that Tax-mediated inhibition of STAT2 transactivation is not due to an impairment of the general transcription machinery in Tax-expressing cells. Additionally, this result further excluded the possibility that Tax-mediated inhibition of ISGF3-directed transcription was attributable to the perturbation of events such as nuclear translocation because both GAL4-Stat2(TA) and GAL4-VP16 utilizes the same nuclear localization signal of GAL4. Taken together, these results suggest that Tax protein inhibits IFN-α signaling via repressing STAT2 transactivation.

Tax down-modulates IFN-α signaling by competitive binding to CBP/p300 coactivator

It has been demonstrated that STAT2 and STAT2-containing ISGF3 function in transcriptional activation partly through recruitment of CBP/p300 (Bhattacharya et al., 1996). Likewise, Tax also utilizes CBP/p300 for implementing its transcriptional activation competence, and moreover, Tax has been shown to inhibit CBP/p300-mediated transcription by competitive usage of the coactivator. Accordingly, a possible mechanism for Tax-mediated inhibition of IFN-α-activated ISGF3 transactivation is through binding to CBP/p300 in competition with STAT2. If it is true, the binding ability of Tax to CBP/p300 should be crucial for its repression of ISGF3 transactivation. To test this hypothesis, we investigated whether the mutant TaxK88A, defective in CBP/p300 binding, could exert similar repressive effect on ISGF3-directed transcription. As shown in Fig. 4A, the inhibitory effect of Tax on IFN-α-stimulated luciferase expression from pISRE-luc was completely abrogated by the mutation introduced in TaxK88A, revealing a correlation between CBP/p300-binding and ISGF3 repression. Similar result was obtained from the reporter assay with pGAL4-Stat2(TA) and pGAL4-luc, confirming that the binding of Tax to CBP/p300 is responsible for the inhibition of STAT2 and ISGF3 transactivation by Tax. Comparable expression of Tax and TaxK88A in each transfectant was confirmed by Western blot analysis (Fig. 4B).

To further verify the hypothesis that competition for limiting CBP/p300 is a mechanism for the observed Tax-mediated ISGF3 inhibition, we

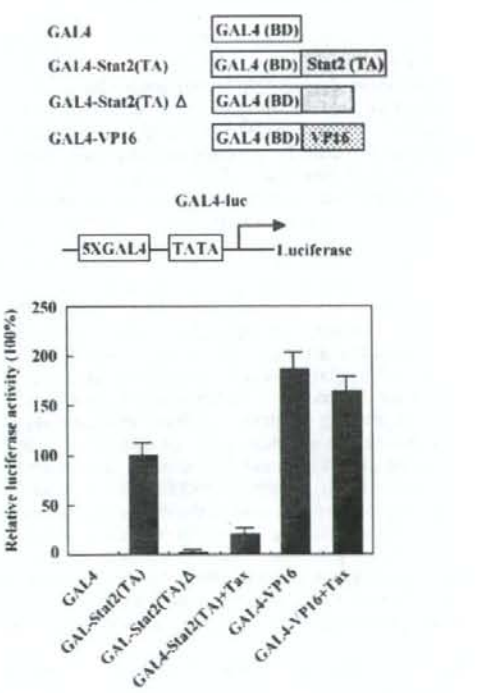

Fig. 3. Inhibition of STAT2 transactivation function by Tax. GAL4 carries the DNA binding domain only; GAL4-Stat2(TA) and GAL4-VP16 contain the transactivation domain of STAT2 and VP16 fused directly with the binding domain of GAL4; GAL4-Stat2(TA)Δ is a mutant of GAL4-Stat2(TA) with C-terminal 83 amino acids of STAT2 deleted. HeLa cells were transfected with the indicated expression constructs together with the GAL4-luc reporter vector, and luciferase activities were determined and calculated as described for Fig. 1. The results are from four independent triplicate experiments.

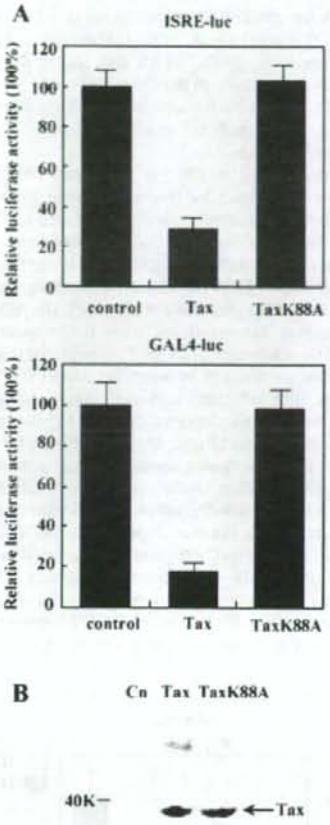

Fig. 4. Tax's ability to bind to CBP is critical for its repressive effect on STAT2 transactivation. (A) Huh-7 cells were transfected with ISRE-luc (upper) or GAL4-luc (lower) together with pCn, pCnwtax or pCnTaxK88A. Mutant TaxK88A harbors an amino acid substitution at condon 88 from lysine to alanine and is defective in CBP/p300 binding. Cells were treated with 100 IU/ml of human IFN-α 24 h later, and the luciferase activity was measured following a further incubation for 24 h. Renilla luciferase activities from cotransfected pRL-TK were used to normalize the transfection efficiency. Normalized luciferase activity from an otherwise identical control transfection with pCn vector was set as 100%, and those in other transfectants are expressed as relative percentage. Representative data are from five independent triplicate transfections. (B) Similar level of Tax expression in cells transfected with pCnwtax or pCnTaxK88A. Cells transfected with each indicated construct were harvested 48 h posttransfection, and Western blot analysis was performed using anti-Tax antibody (AS-5703). Solid arrow indicates the signals of Tax protein.

next investigated whether exogenously expressed CBP/p300 could restore the reduced ISGF3 transcriptional activity by Tax. In the absence of Tax, expression of p300 enhanced ISRE-directed luciferase gene expression in response to IFN-α (Fig. 5A), indicating a rate limiting level of p300 within the nucleus. Noteworthily, cotransfection of p300 expression plasmid completely restored the Tax-mediated inhibition of ISGF3 transactivation. Western blot analysis showed a similar Tax expression in Huh-7 cells irrespective of whether p300 was expressed or not (Fig. 5B), excluding the possibility that derepression of ISGF3 function by overexpression of p300 is due to reduced Tax expression in cells overexpressing p300. Together, these results strongly suggest that Tax-mediated inhibition of ISGF3 transactivation potential is mediated by competitive usage of CBP/p300 between Tax and STAT2.

Competition between Tax and STAT2 for p300 binding

To provide further evidence supporting the competition model proposed above, we next determined whether Tax could bind to p300 in competition with STAT2 in vitro. GST pull-down assay was performed using the GST-p300$^{302-661}$ fusion protein containing GST fused to amino acids 302–661 of p300, which encompasses the homologous region of the CH1 and KIX domains of CBP. Purified GST-p300$^{302-661}$ was bound to glutathione-agarose beads and then incubated with labeled in vitro translated Tax or STAT2 protein. Purified GST was included as a negative control. As expected, either Tax or STAT2 bound well to GST-p300$^{302-661}$ (Fig. 6, lanes 3–4), while no interaction was detected with GST alone (Fig. 6A, lanes 1–2). Notably, inclusion of increasing amount of purified Tax protein in the binding mixture dose-dependently reduced STAT2 binding to GST-p300$^{302-661}$ (Fig. 6A, lanes 5–7). This finding indicates that Tax competes with STAT2 for binding to p300. To exclude the possibility that Tax could interact directly with STAT2 and thereby prevent STAT2 from binding to p300, the binding mixture was subject to immunoprecipitation with anti-Tax antibody. STAT2 was not co-precipitated with anti-Tax antibody (Fig. 6B, upper), whereas association of p300 with Tax was detected under the same condition (Fig. 6B, lower), indicating that Tax did not directly interact with STAT2. Together, these data support a competition between Tax and STAT2 for p300 binding, which may account for the observed repression of STAT2 by Tax.

Tax-mediated inhibition of JAK-STAT signaling is specific for IFN-α

In addition to STAT2, STAT1 has also been shown to interact with CBP/p300, which plays a role in IFN-γ-induced signal transduction. To address whether Tax might affect IFN-γ signaling via competition with STAT1 for binding to CBP/p300, Tax-expressing plasmid was transfected into Jurkat T cells together with pGAS-luc, a reporter

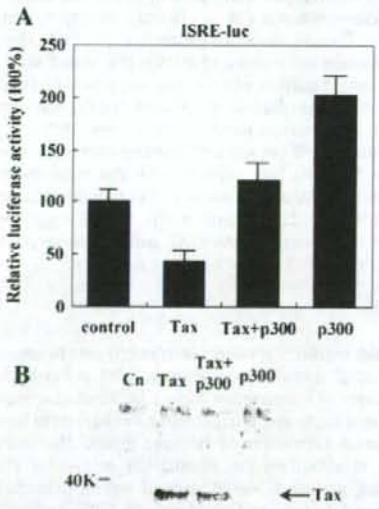

Fig. 5. Tax-mediated inhibition of STAT2 transactivation was reversed by overexpression of p300. (A) ISRE-luc reporter vector was transfected into Huh-7 cells together with pCn, pCnwtax and/or p300. Relative luciferase activities were determined and calculated as described for Fig. 1. Representative results are from three independent triplicate transfections. (B) Comparable Tax expression in cells irrespective of p300 co-expression was confirmed by Western blot analysis.

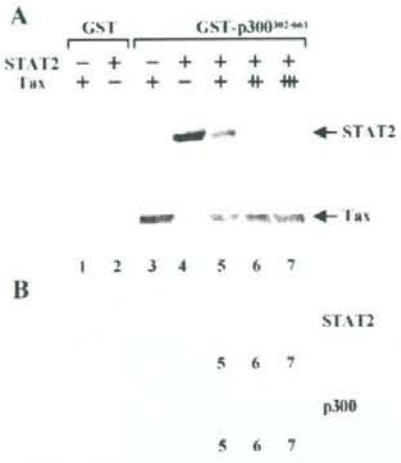

Fig. 6. (A) Tax inhibits STAT2 binding to p300. Labeled STAT2 or Tax in vitro translation product was incubated with GST alone (lanes 1–2) or GST-p300$^{302-661}$ (lanes 3–4). In competition assay (lanes 5–7), STAT2 was incubated with GST-p300$^{302-661}$ in the presence of increasing amount of Tax. (B) Tax does not directly interact with STAT2. The same reaction mixture was immunoprecipitated with anti-Tax antibody followed by Western blotting with anti-Stat2 (upper) or anti-p300 (lower) antibody.

vector encoding the luciferase gene under the control of tandem repeats of gamma-activated sequence (GAS) element that is recognized by STAT1 homodimer induced by IFN-γ. Cells were cultured in the absence or presence of 500 IU/ml of human IFN-γ 24 h later, and the luciferase activity was measured after an additional incubation for 24 h. As shown in Fig. 7A, the luciferase expression was significantly induced by treatment with IFN-γ, indicating the presence of functional IFN-γ receptor and STAT1 in Jurkat T cells. IFN-γ-induced luciferase expression was not significantly affected by cotransfection with either Tax- or TaxK88A-expressing plasmid. The luciferase expression under the control of HTLV-I LTR, which was monitored under the same condition, was substantially stimulated by cotransfection of Tax expression plasmid, suggesting that Tax was expressed and its function was intact in Jurkat T cells treated with IFN-γ (Fig. 7B). Further, expression of Tax was confirmed by immunoprecipitation and subsequent Western blot analysis with the antibody respectively recognizing the N and C terminus of Tax protein (data not shown). Together with the data shown in Fig. 1, it is suggested that Tax specifically modulates the JAK-STAT pathway in respond to IFN-α while having no effect on the signaling via IFN-γ.

Discussion

CBP/p300 regulates a variety of transcription factors involved in multiple signal transduction pathways, and competition between various classes of transcription factors for limiting amounts of CBP/p300 has been suggested as a repression mechanism to coordinate the transcriptional regulation of relevant genes. The transcriptional outcomes of simultaneous stimulation of two or more signal transduction pathways would depend on the abundance of the transcriptional factors and their relative affinities for CBP/p300. Inhibition of Ap1-dependent gene activation by steroid receptors and STAT1, for example, has been demonstrated to be attributable to competitive usage of CBP/p300 (Horvai et al., 1997; Kamei et al., 1996). Similarly, several oncogenic viruses encode viral proteins that bind to CBP/p300 and consequently deregulate CBP/p300-mediated transcription. HTLV-1-encoded Tax protein is among the best known of these. Indeed, multiple studies have linked Tax's binding to CBP/p300 with its repressive effect on the transcription directed by p53 (Ariumi et al., 2000), p73 (Ogryzko et al., 1996), c-Myb (Dai et al., 1996), and c-Jun (Van Orden et al., 1999), which also utilize CBP/p300 as the coactivator. Tax deregulation of the CBP/p300-mediated transcription, most of which are involved in apoptosis, cell cycle regulation, and differentiation, has significant implication in HTLV-1-associated malignant transformation.

Here, we investigated the effect of Tax protein on IFN-α-mediated signal pathway. Precedence for this study comes from our previous observation showing an attenuated IFN-α-induced antiviral response in Tax-expressing cells (Zhang et al., 2007), providing an explanation for the clinical study revealing a significantly lower rate of sustained IFN-α response in HCV/HTLV co-infected individuals, relative to those infected with HCV alone (Kishihara et al., 2001). The results presented here indicate that Tax interferes with IFN-α-induced JAK-STAT pathway, and the molecular basis for Tax-mediated IFN-α inhibition appears to be the competition between Tax and STAT2 for coactivator CBP/p300. We inferred this conclusion based on the following observations. Firstly, Tax's abilities to activate CREB-dependent pathway (Fig. 1A) and to bind CBP (Fig. 4A) are necessary for its repression on ISGF3-directed transcription. Secondly, in the presence of Tax, the formation of DNA-binding ISGF3 complex is unaffected (Fig. 2A) nevertheless being functionally compromised in directing ISRE-driven gene expression. Thirdly, Tax dose-dependently inhibits the binding of STAT2 to p300 in vitro (Fig. 6A), and there is no direct interaction between Tax and STAT2 in immunoprecipitation assay (Fig. 6B). Finally, Tax also inhibits the transcriptional activity of GAL4-Stat2(TA) containing the transactivation domain of STAT2 fused with GAL4 DNA-binding domain (Fig. 3), and Tax repression on ISGF3 was restored by

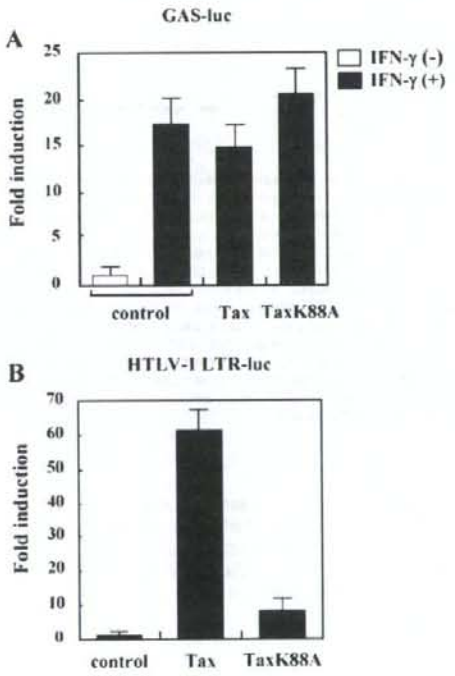

Fig. 7. Tax does not affect JAK–STAT pathway in response to IFN-γ signaling. Jurkat T cells were transfected with GAS-luc (A) or HTLV-1 LTR-luc (B) along with pCn, pCnwtax or pCnTaxK88A. Relative luciferase activities were determined as described for Fig. 1. Fold induction means the luciferase activity relative to that co-transfected with the control vector pCn. The results are from three independent triplicate experiments.

overexpression of p300 (Fig. 5A). Together, these findings strongly suggest that Tax competitively binds to CBP/p300 and disables its function in ISGF3-directed transcription.

Tax m319, which corresponds to the previously characterized M47 Tax mutant (Smith and Greene 1990), contains two amino acid mutations (L319R and L320S) in the carboxy-terminal domain. While Harrod et al. (1998) identified the KID-like domain around amino acid residues 81–95 as the major CBP-binding domain of Tax, Bex et al. (1998) reported that M47 mutant is impaired in CBP binding, thus explaining its inability to activate CREB pathway. A compromised interpretation is that the KID-like domain in Tax is critical for the recruitment of CBP/p300 but additional contact(s) might also be required for interaction of Tax with CBP/p300. Alternatively, the carboxy-terminal domain might play a role in maintaining the overall structure and/or promoting the conformational change to render the KID-like domain accessible to CBP/p300. If this is the case, the mutations in Tax m319 might attenuate the ability of Tax to sequester CBP/p300, thereby failing to suppress ISRE-luc expression. Actually, a similar observation was previously reported by Ariumi et al. (2000), who demonstrated that the mutations in Tax m319 abrogated the ability of Tax to repress p53-directed transcription by competitive binding to CBP. Further studies are now in progress to clarify this issue.

Repression of STAT2 by Tax is reminiscent of the scenario described in adenovirus-encoded E1A protein, which has been demonstrated to repress STAT2 transactivation and IFN-α-induced transcription at least in part through competition for CBP/p300 (Bhattacharya et al., 1996). In addition to these two viruses, viral proteins encoded by other oncogenic viruses, such as large T antigen from SV40 (Eckner et al., 1996) and polyomavirus (Cho et al., 2001), E6 protein from human papillomavirus (Patel et al., 1999), and Tat protein from HIV-1 (Ott et al., 1999), also bind to CBP/p300 and deregulate CBP/p300-mediated cellular transcription, it is thus probable, but remains to be proven, that an analogous anti-IFN strategy might also be employed by these viruses. It is known that interaction of Tax with the KIX domain of CBP/p300 is crucial for Tax-mediated coactivator recruitment, although additional contacts may further strengthen the interaction and contribute to Tax's transcription function. In the case of STAT2, previous studies have identified the CH1 domain as the binding site (Bhattacharya et al., 1996). CH1 domain is located immediately amino-terminal to the KIX domain. It is thus possible that steric hindrance or conformational changes following binding of Tax to CBP/p300 might result in the diminishment of STAT2 binding by blocking access of STAT2 to its binding sites. Additionally, it was reported that the transcriptional repression between Tax and p73β, c-Myb, c-Jun pathway is reciprocal (Lemasson and Nyborg, 2001; Van Orden et al., 1999). In a reporter assay to investigate whether STAT2 similarly repress Tax function, however, we found that overexpression of STAT2 didn't obviously affect Tax-stimulated HTLV-1 transcription (data not shown), suggesting that STAT2 could not inhibit binding of Tax to CBP/p300 and affect its ability to function as a coactivator in conjunction with CREB transcription factor. The failure of STAT2 to displace Tax from CBP/p300 is probably due to a higher affinity of Tax than STAT2 for CBP/p300. Alternatively, KIX domain may remain accessible for Tax binding and STAT2 displacement after binding of STAT2 to CH1 domain. Actually, a similar observation was previously reported by Riou et al., who demonstrated that Tax represses MyoD-dependent transcription by inhibiting MyoD-binding to the KIX domain of p300, but not vice versa (Riou et al., 2000). On the contrary, co-transfection of STAT2-expressing plasmid significantly inhibited Tax stimulation of HIV-1 transcription (data not shown), which involves activation of NF-κB pathway by Tax. Binding of STAT2 to CBP/p300 affects its ability to function as a coactivator in NF-κB- but not in CREB-dependent transcription, which may not be surprising considering that STAT2 binds to CH1 domain distinct from Tax and CREB, whereas both STAT2 and RelA of NF-κB share a common binding site (CH1) on CBP/p300. Consistent with this observation, binding of STAT2 to p300 in competition with RelA was demonstrated as the mechanism by which IFN-α inhibited TNF-α stimulation of HIV gene expression via NF-κB (Hottiger et al., 1998).

The data presented here indicate that Tax specifically deregulated the JAK-STAT pathway in respond to IFN-α but having no effect on the signaling via IFN-γ, suggesting that Tax did not interfere with the recruitment of CBP by STAT1. This is probably attributable to the fact that STAT1 interacts with the CH3 domain of CBP/p300 (Zhang et al., 1996), a region is relatively far from the binding site of Tax (KIX domain), and the CH3 domain may remain accessible for STAT1 binding after binding of Tax to KIX domain. Also, an alternative explanation for the different effects of Tax on IFN-α and IFN-γ signaling might be due to the difference in affinity of STAT2 and STAT1 for CBP/p300 binding, relative to that of Tax.

The ability of Tax to inhibit ISGF3 transactivation has potential biological implications. Like IFN-γ, IFN-α also plays a critical role in cancer immunosurveillance and immunoediting (Dunn et al., 2005). Impaired IFN-α signaling might therefore result in a loss of both the normal control of proliferation and regulation of apoptosis, thereby increasing the malignant behavior (Matin et al., 2001; Picaud et al., 2002). Indeed, reduced IFN-α-responsiveness has been linked to malignancy in various cancer types. For example, it was reported that deficiency in ISGF3 activity, due to suppressed expression of one or more components of ISGF3 complex, was involved in the pathogenesis of squamous cell carcinoma of the skin (Clifford et al., 2002). Further, it was demonstrated that stable expression of dominant negative STAT2 suppressed IFN-α-induced growth inhibitory response in highly IFN-α-sensitive human cells (Clifford et al., 2003). It is thus conceivable that repression of ISGF3 transactivation by Tax could contribute to the HTLV-1-associated malignancy by conferring a growth and/or survival advantage. Consistent with this hypothesis, it was previously reported that HTLV-1-infected T cells evade the antiproliferative action of IFN-β while having normal level of IFNAR1 expression and STAT phosphorylation (Smith et al., 1999). Additionally, ISGF3-directed transcription is a crucial step in transducing IFN-α-mediated antiviral response. The data presented here suggest that Tax-mediated ISGF3 inhibition might lead to a global repression of antiviral defense gene expression, thereby rendering unhindered viral replication. In addition to facilitating the replication of HTLV-1 itself, the antagonistic effect of Tax on IFN might also modulate the replication of other co-existing viral pathogens, providing a possible mechanism for the severer clinical consequence of viral infectious disease and poorer IFN-α responsiveness in patients co-infected with HTLV-1 (Boschi-Pinto et al., 2000; Kishihara et al., 2001). However, one concern in interpreting the physiological relevance of the results obtained here is that the level of Tax expression in HTLV-1-infected patients may be lower than that in established cell lines used here. In view that the titrating study was not performed here, it thus cannot be ruled out that Tax-mediated anti-IFN effect might be milder in vivo than that observed here.

While the manuscript was being prepared, Feng and Ratner reported that HTLV-1 down-regulates IFN-α-stimulated JAK-STAT signaling by reducing phosphorylation of tyrosine kinase 2 and STAT2, and provided evidence suggesting that Gag or Pr may be responsible for HTLV-1-mediated IFN-α inhibition (Feng and Ratner, 2008). Our data, however, do not support that Tax perturbs the events involved in the formation of DNA-binding ISGF3 complex. As shown in the result of EMSA (Fig. 2A), IFN-α-induced ISGF3 formation in Huhwtax was similar to that detected in HuhCn cells. Huhwtax constitutively expresses Tax protein at a level comparable to that in HTLV-1-infected MT-2 cells (Fig. 2B), and moreover this level of Tax expression conferred an attenuated IFN-α-induced antiviral response in Huhwtax cells (Zhang et al., 2007). Thus, the possibility that unaffected formation of ISRE-binding ISGF3 complex in Huhwtax was due to insufficient Tax expression in these cells was largely lessened, if could not be ruled out completely, allowing us to infer that Tax inhibits IFN-α signaling via a mechanism other than derailing the events involved in the formation of DNA-binding ISGF3 complex.

Nonetheless, the data presented here are not contradictory to the conclusion drawn from the Ratner's study, and it is possible that different HTLV gene products may act at different level of the JAK-STAT signaling to counteract IFN's action. Actually, it is frequently that viruses employ more than one strategy to evade IFN system.

In conclusion, we investigated here the effect of HTLV-1-encoded Tax protein on IFN-α signaling pathway, and provide evidence demonstrating that Tax negatively modulates IFN-α-induced JAK-STAT pathway by competing with STAT2 for coactivator CBP/p300. Tax preventing IFN-α from inducing an antiviral state and programming cell death provides an additional mechanism for the role of Tax in persistent viral infection and development of ATLL in HTLV-1-infected individuals, highlighting the significance of the anti-HTLV strategies targeting Tax protein.

Materials and methods

Plasmids

Empty plasmid pCn, and plasmids encoding wild-type HTLV Tax (pCnwtax) or its mutants (pCnm148 and pCnm319, K88A) have all been described previously (Yamaoka et al; 1996; Zhang et al., 2007; Harrod et al., 1998). The reporter vectors, pISRE-luc and pGAS-luc, were purchased from Stratagene. For construction of pGAL4-Stat2(TA), the cDNA of STAT2 transactivation domain (amino acids 670–851) was amplified with primers 5′-atctgcgatcgccatgCGGGATGAAGCTTTT-GGGTG-3′ and 5′-acctgtttaaacCTAGAAGTCAGAAGGCAT-3′, digested with Sgf I and Pme I, and ligated into in pFN11A(BIND) Flexi vector (Promega), which had been cut with the same enzymes immediate downstream of GAL4 DNA-binding domain. The cDNA insert for pGEX-p300 (amino acids 302–661) was generated by PCR using primers 5′-ataggatccatgGGTCAACAGCCAGCCCCG-3′ and 5′-agagaattctcaAG-CATTTGGTAGCATGTTCTG-3′, digested with BamH I and EcoR I and ligated into BamH I/EcoR I-digested pGEX-2Z (Amersham). The sequences of these constructs were confirmed by nucleotide sequencing.

Cells

Human hepatoma cell line Huh-7 and human cervical carcinoma HeLa cells were purchased from the American Type Culture Collection (ATCC) and maintained in Dulbecco's modified Eagle's medium (DMEM, Invitrogen) supplemented with 10% fetal calf serum and 50 U/ml penicillin and streptomycin. Jurkat T-lymphocytes were maintained in RPMI1640 medium supplement with 15% fetal calf serum. The cell line Huhwtax, which stably expresses Tax at a level comparable to HTLV-1-infected MT-2 cells, was established by transfecting Huh-7 cells with pCnwtax followed by G418 selection and limiting dilution.

Transient transfection and luciferase assay

Cells were seeded at 1×10^5 in 1 ml medium per well of 12-well plates 24 h before transfection. Indicated plasmid DNAs were transfected into cells with FuGENE6 (Roche). For each transfection, pRL-TK (Promega) vector was cotransfected as an internal control to normalize the transfection efficiency. The cells were harvested at 48 h posttransfection, and the cell lysates were prepared for luciferase assays with Dual-Luciferase Reporter Assay System (Promega) according to the manufacturer's instruction. Luciferase activities were measured using a TD-20/20 Luminometer (Promega).

EMSA

The probe used in the EMSA was obtained by annealing biotinylated consensus ISRE oligonucleotides $(AGGAAATAGAAACTG)_2$ and its complement. Nuclear extracts were prepared from the cells treated with or without IFN-α using NE-PER Nuclear and Cytoplasmic Extraction Reagent Kit (Pierce). EMSA was performed with the Lightshift Chemiluminescent EMSA Kit (Pierce) and the signals were detected with streptavidin-horseradish peroxidase conjugate and chemiluminescent substrate. For competition experiments, unlabeled double-strand oligonucleotides were used in a 50-fold molar excess. For supershift experiments, nuclear extracts were pre-incubated for 30 min with specific antibodies before addition to the binding reaction.

GST pull-down assay

GST-$p300^{302-661}$ fusion protein was induced by isopropyl-thiogalactopyranoside in BL21 *Escherichia coli* transformed with pGEX-p300, purified by binding to glutathione-Sepharose 4B (Bulk GST Purification Module, GE Healthcare), and dialyzed with PBS overnight. Tax and STAT2 proteins were in vitro translated with the TNT-coupled reticulocyte lysate systems kit (Promega) and labeled with Transcend tRNA (Promega). GST or GST-$p300^{302-661}$ was incubated with Tax or STAT2 in binding buffer. GS4B beads were added and incubated for 1 h. Proteins that bound to the beads were separated by SDS/PAGE and detected with streptavidin-horseradish peroxidase and chemiluminescent substrate.

Western blot analysis

Separation of protein on sodium dodecyl sulfate-polyacrylamide gel electrophoresis followed standard methods. After the proteins were transferred to Hybond-P PVDV Membrane (GE Healthcare), the membranes were blocked and then probed with monoclonal antibody specific for HTLV-I Tax (AS-5703, Microbix Biosystems Inc.), and signals were visualized with ECL Plus Western Blotting Detection Reagents (GE Healthcare).

References

Ariumi, Y., Kaida, A., Lin, J.Y., Hirota, M., Masui, O., Yamaoka, S., Taya, Y., Shimotohno, K., 2000. HTLV-1 tax oncoprotein represses the p53-mediated trans-activation function through coactivator CBP sequestration. Oncogene 19 (12), 1491–1499.

Bannister, A.J., Kouzarides, T., 1996. The CBP co-activator is a histone acetyltransferase. Nature 384 (6610), 641–643.

Bex, F., Yin, M.J., Burny, A., Gaynor, R.B., 1998. Differential transcriptional activation by human T-cell leukemia virus type I Tax mutants is mediated by distinct interaction with CREB binding protein and p300. Mol. Cell. Biol. 18 (4), 2392–2405.

Bhattacharya, S., Eckner, R., Grossman, S., Oldread, E., Arany, Z., D'Andrea, A., Livingston, D.M., 1996. Cooperation of Stat2 and p300/CBP in signalling induced by interferon-alpha. Nature 383 (6598), 344–347.

Boschi-Pinto, C., Stuver, S., Okayama, A., Trichopoulos, D., Orav, E.J., Tsubouchi, H., Mueller, N., 2000. A follow-up study of morbidity and mortality associated with hepatitis C virus infection and its interaction with human T lymphotropic virus type I in Miyazaki, Japan. J. Infect. Dis. 181 (1), 35–41.

Cho, S., Tian, Y., Benjamin, T.L., 2001. Binding of p300/CBP co-activators by polyoma large T antigen. J. Biol. Chem. 276 (36), 33533–33539.

Chrivia, J.C., Kwok, R.P., Lamb, N., Hagiwara, M., Montminy, M.R., Goodman, R.H., 1993. Phosphorylated CREB binds specifically to the nuclear protein CBP. Nature 365 (6449), 855–859.

Clifford, J.L., Walch, E., Yang, X., Xu, X., Alberts, D.S., Clayman, G.L., El-Naggar, A.K., Lotan, R., Lippman, S.M., 2002. Suppression of type I interferon signaling proteins is an early event in squamous skin carcinogenesis. Clin. Cancer Res. 8 (7), 2067–2072.

Clifford, J.L., Yang, X., Walch, E., Wang, M., Lippman, S.M., 2003. Dominant negative signal transducer and activator of transcription 2 (STAT2) protein: stable expression blocks interferon alpha action in skin squamous cell carcinoma cells. 2003. Mol. Cancer Ther. 2 (5), 453–459.

Dai, P., Akimaru, H., Tanaka, Y., Hou, D.X., Yasukawa, T., Kanei-Ishii, C., Takahashi, T., Ishii, S., 1996. CBP as a transcriptional coactivator of c-Myb. Genes Dev. 10 (5), 528–540.

Dunn, G.P., Bruce, A.T., Sheehan, K.C., Shankaran, V., Uppaluri, R., Bui, J.D., Diamond, M.S., Koebel, C.M., Arthur, C., White, J.M., Schreiber, R.D., 2005. A critical function for type I interferons in cancer immunoediting. Nat. Immunol. 6 (7), 722–729.

Eckner, R., Ewen, M.E., Newsome, D., Gerdes, M., DeCaprio, J.A., Lawrence, J.B., Livingston, D.M., 1994. Molecular cloning and functional analysis of the adenovirus E1A-associated 300-kD protein (p300) reveals a protein with properties of a transcriptional adaptor. Genes Dev. 8 (8), 869–884.

Eckner, R., Ludlow, J.W., Lill, N.L., Oldread, E., Arany, Z., Modjtahedi, N., DeCaprio, J.A., Livingston, D.M., Morgan, J.A., 1996. Association of p300 and CBP with simian virus 40 large T antigen. Mol. Cell. Biol. 16 (7), 3454–3464.

Feng, X., Ratner, L., 2008. Human T-cell leukemia virus type 1 blunts signaling by interferon alpha. Virology 374 (1), 210–216.
Gessain, A., Barin, F., Vernant, J.C., Gout, O., Maurs, L., Calender, A., de The, G., 1985. Antibodies to human T-lymphotropic virus type-I in patients with tropical spastic paraparesis. Lancet 2 (8353), 407–410.
Giebler, H.A., Loring, J.E., van Orden, K., Colgin, M.A., Garrus, J.E., Escudero, K.W., Brauweiler, A., Nyborg, J.K., 1997. Anchoring of CREB binding protein to the human T-cell leukemia virus type 1 promoter: a molecular mechanism of Tax transactivation. Mol. Cell. Biol. 17 (9), 5156–5164.
Gill, P.S., Harrington Jr., W., Kaplan, M.H., Ribeiro, R.C., Bennett, J.M., Liebman, H.A., Bernstein-Singer, M., Espina, B.M., Cabral, L., Allen, S., Kornblau, S., Pike, M.C., Levine, A.M., 1995. Treatment of adult T-cell leukemia-lymphoma with a combination of interferon alfa and zidovudine. N. Engl. J. Med. 332 (26), 1744–1748.
Grassmann, R., Dengler, C., Müller-Fleckenstein, I., Fleckenstein, B., McGuire, K., Dokhelar, M.C., Sodroski, J.G., Haseltine, W.A., 1989. Transformation to continuous growth of primary human T lymphocytes by human T-cell leukemia virus type I X-region genes transduced by a Herpesvirus saimiri vector. Proc. Natl. Acad. Sci. U.S.A. 86 (9), 3551–3555.
Grassmann, R., Berchtold, S., Radant, I., Alt, M., Fleckenstein, B., Sodroski, J.G., Haseltine, W.A., Ramstedt, U., 1992. Role of human T-cell leukemia virus type 1 X region proteins in immortalization of primary human lymphocytes in culture. J. Virol. 66 (7), 4570–4575.
Harrod, R., Tang, Y., Nicot, C., Lu, H.S., Vassilev, A., Nakatani, Y., Giam, C.Z., 1998. An exposed KID-like domain in human T-cell lymphotropic virus type 1 Tax is responsible for the recruitment of coactivators CBP/p300. Mol. Cell. Biol. 18 (9), 5052–5061.
Hermine, O., Bouscary, D., Gessain, Turlure, P., Leblond, V., Franck, N., Buzyn-Veil, A., Rio, B., Macintyre, E., Dreyfus, F., Bazarbachi, A., 1995. Treatment of adult T-cell leukemia-lymphoma with zidovudine and interferon alfa. N. Engl. J. Med. 332 (26), 1749–1751.
Horvai, A.E., Xu, L., Korzus, E., Brard, G., Kalafus, D., Mullen, T.M., Rose, D.W., Rosenfeld, M.G., Glass, C.K., 1997. Nuclear integration of JAK/STAT and Ras/AP-1 signaling by CBP and p300. Proc. Natl. Acad. Sci. U.S.A. 94 (4), 1074–1079.
Hottiger, M.O., Felzien, L.K., Nabel, G.J., 1998. Modulation of cytokine-induced HIV gene expression by competitive binding of transcription factors to the coactivator p300. EMBO J. 17 (11), 3124–3134.
Janknecht, R., Hunter, T., 1996. Transcription. A growing coactivator network. Nature 383 (6595), 22–23.
Kamei, Y., Xu, L., Heinzel, T., Torchia, J., Kurokawa, R., Gloss, B., Lin, S.C., Heyman, R.A., Rose, D.W., Glass, C.K., Rosenfeld, M.G., 1996. A CBP integrator complex mediates transcriptional activation and AP-1 inhibition by nuclear receptors. Cell 85 (3), 403–414.
Kishihara, Y., Furusyo, N., Kashiwagi, K., Mitsutake, A., Kashiwagi, S., Hayashi, J., 2001. Human T lymphotropic virus type 1 infection influences hepatitis C virus clearance. J. Infect. Dis. 184 (9), 1114–1119.
Kwok, R.P., Laurance, M.E., Lundblad, J.R., Goldman, P.S., Shih, H., Connor, L.M., Marriott, S.J., Goodman, R.H., 1996. Control of cAMP-regulated enhancers by the viral transactivator Tax through CREB and the co-activator CBP. Nature 380 (6575), 642–646.
Lemasson, I., Nyborg, J.K., 2001. Human T-cell leukemia virus type I tax repression of p73beta is mediated through competition for the C/H1 domain of CBP. J. Biol. Chem. 276 (19), 15720–15727.
Matin, S.F., Rackley, R.R., Sadhukhan, P.C., Kim, M.S., Novick, A.C., Bandyopadhyay, S.K., 2001. Impaired alpha-interferon signaling in transitional cell carcinoma: lack of p48 expression in 5637 cells. Cancer Res. 61 (5), 2261–2266.
Ogryzko, V.V., Schiltz, R.L., Russanova, V., Howard, B.H., Nakatani, Y., 1996. The transcriptional coactivators p300 and CBP are histone acetyltransferases. Cell 87 (5), 953–959.
Osame, M., Usuku, K., Izumo, S., Ijichi, N., Amitani, H., Igata, A., 1986. HTLV-I associated myelopathy, a new clinical entity. Lancet 1 (8488), 1031–1032.
Ott, M., Schnölzer, M., Garnica, J., Fischle, W., Emiliani, S., Rackwitz, H.R., Verding, E., 1999. Acetylation of the HIV-1 Tat protein by p300 is important for its transcriptional activity. Curr. Biol. 9 (24), 1489–1492.
Patel, D., Huang, S.M., Baglia, L.A., McCance, D.J., 1999. The E6 protein of human papillomavirus type 16 binds to and inhibits co-activation by CBP and p300. EMBO J. 18 (18), 5061–5072.
Picaud, S., Bardot, B., De Maeyer, E., Seif, I., 2002. Enhanced tumor development in mice lacking a functional type I interferon receptor. J. Interferon Cytokine Res. 22 (4), 457–462.
Riou, P., Bex, F., Gazzolo, L., 2000. The human T cell leukemia/lymphotropic virus type 1 Tax protein represses MyoD-dependent transcription by inhibiting MyoD-binding to the KIX domain of p300. A potential mechanism for Tax-mediated repression of the transcriptional activity of basic helix-loop-helix factors. J. Biol. Chem. 275 (14), 10551–10560.
Smith, D., Buckle, G.J., Hafler, D.A., Frank, D.A., Hollsberg, P., 1999. HTLV-I-infected T cells evade the antiproliferative action of IFN-beta. Virology 257 (2), 314–321.
Smith, M.R., Greene, W.C., 1990. Identification of HTLV-I tax trans-activator mutants exhibiting novel transcriptional phenotypes. Genes Dev. 4 (11), 1875–1885.
Sun, W.H., Pabon, C., Alsayed, Y., Huang, P.P., Jandeska, S., Uddin, S., Platanias, L.C., Rosen, S.T., 1998. Interferon-alpha resistance in a cutaneous T-cell lymphoma cell line is associated with lack of STAT1 expression. Blood 91 (2), 570–576.
Van Orden, K., Giebler, H.A., Lemasson, I., Gonzales, M., Nyborg, J.K., 1999. Binding of p53 to the KIX domain of CREB binding protein. A potential link to human T-cell leukemia virus, type I-associated leukemogenesis. J. Biol. Chem. 274 (37), 26321–26328.
Yamaoka, S., Inoue, H., Sakurai, M., Sugiyama, T., Hazama, M., Yamada, T., Hatanaka, M., 1996. Constitutive activation of NF-kB is essential for transformation of rat fibroblasts by the human T-cell leukemia virus type I Tax protein. EMBO J. 15 (4), 873–887.
Yang, X.J., Ogryzko, V.V., Nishikawa, J., Howard, B.H., Nakatani, Y., 1996. A p300/CBP-associated factor that competes with the adenoviral oncoprotein E1A. Nature 382 (6589), 319–324.
Yoshida, M., Seiki, M., Yamaguchi, K., Takatsuki, K., 1984. Monoclonal integration of human T-cell leukemia provirus in all primary tumors of adult T-cell leukemia suggests causative role of human T-cell leukemia virus in the disease. Proc. Natl. Acad. Sci. U.S.A. 81 (19), 2534–2537.
Zhang, J.J., Vinkemeier, U., Gu, W., Chakravarti, D., Horvath, C.M., Darnell Jr., J.E., 1996. Two contact regions between Stat1 and CBP/p300 in interferon gamma signaling. Proc. Natl. Acad. Sci. U.S.A. 93 (26), 15092–15096.
Zhang, J., Yamada, O., Kawagishi, K., Yoshida, H., Araki, H., Yamaoka, S., Hattori, T., Shimotohno, K., 2007. Up-regulation of hepatitis C virus replication by human T cell leukemia virus type I-encoded Tax protein. Virology 369 (1), 198–205.

Characterization of a CD4-independent clinical HIV-1 that can efficiently infect human hepatocytes through chemokine (C-X-C motif) receptor 4

Peng Xiao[a,b], Osamu Usami[a], Yasuhiro Suzuki[a], Hong Ling[b], Nobuaki Shimizu[c], Hiroo Hoshino[c], Min Zhuang[b], Yugo Ashino[a], Hongxi Gu[b] and Toshio Hattori[a]

Objective: HIV-1 isolates are prominently CD4-dependent and, to date, only a few laboratory-adapted CD4-independent strains have been reported. Therefore, whether CD4-independent viruses may exist in HIV-1-infected patients has remained unclear. Here, we report the successful isolation of a CD4-independent clinical HIV-1 strain, designated SDA-1, from the viral quasispecies of a therapy-naive HIV-1 and *Pneumocystis jirovecii* pneumonia patient in the late-stage of AIDS with extremely low CD4 cell count (CD4 = 1/μl). We characterized this virus and further explored whether it could infect or induce pathological effects in human hepatocytes.

Design and methods: To determine coreceptor usage and CD4-independent infection, the HIV-1 envelope (Env)-pseudotypes and Env-chimeric viruses were used.

Results: SDA-1 was able to infect $CD4^-$ cell lines through either chemokine (C-X-C motif) receptor 4 or CCR5. It still maintained the ability to infect $CD4^+$ cells through multiple coreceptors of chemokine (C-X-C motif) receptor 4, chemokine (C-C motif) receptor 5, chemokine (C-C motif) receptor 3 and chemokine (C-C motif) receptor 8. Productive infection by SDA-1 was noted in both CD4-negative hepatoma cells and primary cultured human hepatocytes. Moreover, we demonstrated that SDA-1 could efficiently infect human hepatocytes on both static and mitotic phases through chemokine (C-X-C motif) receptor 4, without inducing apoptotic cell death.

Conclusion: The present study provides evidence that emergence of CD4-independent HIV-1 virus *in vivo* may occur in HIV-1-infected patients. In addition, these results shed light on the mechanisms involved in liver damage in HIV-1-infected individuals, which could have important implications concerning the range of mutability and the pathogenesis of AIDS.

AIDS 2008, **22**:1749–1757

Keywords: CD4-independence, HIV-1, human hepatocytes, human hepatoma cells

Introduction

The entry of HIV-1 into target cells requires interaction of the viral envelope (Env) with CD4 and a chemokine coreceptor [1,2]. Macrophage-tropic HIV-1 viruses primarily use chemokine (C-C motif) receptor 5 (CCR5) (R5) as a coreceptor, whereas T-cell-tropic viruses use chemokine (C-X-C motif) receptor 4

[a]Department of Emerging Infectious Diseases, Division of Internal Medicine, Graduate School of Medicine, Tohoku University, Sendai, Japan, [b]Department of Microbiology, Harbin Medical University, Harbin, China, and [c]Department of Virology and Preventive Medicine, Gunma University School of Medicine, Gunma, Japan.

Correspondence to Toshio Hattori, MD, PhD, Department of Emerging Infectious Diseases, Division of Internal Medicine, Graduate School of Medicine, Tohoku University, Sendai 980-8574, Japan.

Tel: +81 22 717 8220; fax: +81 22 717 8221; e-mail: hattori.t@rid.med.tohoku.ac.jp
Received: 17 January 2008; revised: 21 April 2008; accepted: 9 May 2008.

DOI:10.1097/QAD.0b013e328308937c

(CXCR4) (X4). Dual-tropic viruses (R5X4) use both coreceptors [3]. A few rare viruses can also use alternative coreceptors such as chemokine (C-C motif) receptor 1 (CCR1), chemokine (C-C motif) receptor 2b (CCR2b), chemokine (C-C motif) receptor 8 (CCR8), chemokine (C-X-C motif) receptor 6 (CXCR6), G protein-coupled receptor 1 (GPR1) or GPR15/Bob for entry into coreceptor-transfected $CD4^+$ cell lines [4]. Whatever the coreceptor specificity of an HIV-1 isolate, an interaction with CD4 is always the first step in a chain of events leading to fusion of the viral envelope with the cellular membrane. However, previous studies have shown that SIV [5] and HIV-2 [6] can also infect cells independently of CD4.

In contrast to SIV and HIV-2, HIV-1 CD4-independent viruses are rarely isolated. To date, only a few laboratory CD4-independent HIV-1 variants [7–10] have been reported. Therefore, whether such viruses may exist in HIV-1-infected patients has remained unclear. However, several studies [11–14] have shown that HIV-1-DNA and p24, a core HIV-1 antigen, were detected in CD4-negative cells or tissues such as brain, kidney and liver in HIV-infected individuals, suggesting the possibility that low levels of CD4-independent variants exist *in vivo*. Among such $CD4^-$ cells or tissues, liver is an important organ in determining the prognosis of HIV-1-infected patients. End-stage liver disease is becoming a frequent cause of death in HIV-1-infected hospitalized patients [15–17]. Although the cause of liver injury in HIV-1 patients might be multifactorial, such as hepatitis B virus (HCV) and hepatitis B virus (HBV) coinfection and the side effects of antiretroviral therapy, a number of reports have documented that histological liver abnormalities occurred solely as a result of HIV-1 infection [13,18,19]. Nonetheless, few attempts have been made to elucidate the mechanisms of the liver damage in HIV-1-infected individuals.

In this study, we successfully isolated a CD4-independent clinical HIV-1 strain, designated SDA-1, from the viral quasispecies of a therapy-naive HIV-1 and *Pneumocystis jirovecii* pneumonia (PJP) patient in the late stage of AIDS with extremely low CD4 cell numbers. We characterized the phenotype of this virus and further explored whether it could infect or induce pathological effects in human hepatocytes.

Materials and methods

Patient's information

A 53-year-old Japanese man infected with HIV-1 was admitted to Tohoku University Hospital owing to prolonged fever and severe dyspnea in 2000. His plasma viral load and CD4 cell count at the time of admission was 220 000 copies/ml and 1 cell/μl, respectively. He was diagnosed with PJP, and his clinical stage was classified as IV-C3 [20]. The onset and route of HIV-1 infection were unknown. No evidence of coinfection with HBV or HCV in this patient was found. The patient was treated with trimethoprim and sulfamethoxazole (TMP–SMX) and highly active antiretroviral therapy (HAART). His condition deteriorated rapidly and he died 33 days after admission. Consent for autopsy was denied by the patient's family.

Before HAART, plasma samples and peripheral blood mononuclear cells (PBMC) were collected from this patient and cryopreserved in liquid nitrogen until use. The institutional Ethics Committee approved this study and written informed consent was obtained from the patient.

Virus isolation

HIV-1 isolation was achieved by using an in-vitro short-term phytohemagglutinin (PHA)–PBMC coculture method. Briefly, cryopreserved PBMC (2×10^6) from the patient were cocultivated with PHA-stimulated PBMC (5×10^6) from an HIV-1 seronegative healthy donor. The culture was maintained in RPMI-1640 (Invitrogen, California, USA) containing 10% fetal calf serum and 5 U/ml of recombinant interleukin-2 (IL-2) (Sigma, St. Louis, Missouri, USA). Proliferation of HIV-1 was examined by measuring p24 antigen in the cell culture supernatant using a p24 ELISA kit (RETRO-TEK, ZeptoMetrix Corp., New York, USA). The virus stocks were kept at −80 °C until use.

Amplification of *env* and sequence analysis

The full-length HIV-1 *env* genes were amplified by limiting dilution nested PCR from proviral PBMC DNA or plasma RNA as previously described [21,22]. To avoid artificial recombination and resampling of the viral genomes, independent nested PCR reactions were carried out per specimen [23,24].

The first round PCR was conducted with a F5852–R8935 primer pair (F5852, 5′-TAGAGCCCTGGAAG CATCCAGGAAG, HIV-1 HXB2 nucleotide position 5852–5876; R8935, 5′-TTGCTACTTGTGATTGCT CCATGT, HXB2 nucleotide position 8912–8935). The second round PCR was performed with a F5957–R8903 primer pair (F5957, 5′-GATCGAATTCTAGGCATC TCCTATGGCAGGAAGAAG, HXB2 nucleotide position 5957–5982, containing an additional *Eco*RI site (underlined) to facilitate cloning; R8903, 5′-AGCT CTC GAGGTCTCGAGATACTGCTCCCACCC, HXB2 nucleotide position 8881–8903, containing an additional *Xho*I site (underlined)). The purified PCR products were subcloned into the *Eco*RI and *Xho*I sites of the pSM-HXB2 plasmid. All correctly oriented *env* clones were then screened for biological function [22] followed by sequencing and phylogenetic analysis as previously described [25,26].